(1980).

[4] P. R. Berman, in *Advances in Atomic and Molecular Physics*, edited by D. R. Bates and B. Bederson (Academic, New York, 1977), Vol. 13.

[5] D. G. Steel and R. C. Lind, Opt. Lett. 6, 587 (1981).

[6] NDFWM studies of collision effects using cross-polarized pump and probe show distinctly different behavior from that reported here. J. F. Lam, D. G. Steel, and R. D. McFarlane, to be published.

[7] E. L. Lewis, Phys. Rep. 58, 1 (1980).

Influence of Increasing Nuclear Charge on the Rydberg Spectra of Xe, Cs^+, and Ba^{++}: Correlation, Term Dependence, and Autoionization

W. T. Hill, III
National Bureau of Standards, Washington, D.C. 20234, and Institute for Physical Science and Technology, University of Maryland, College Park, Maryland 20742

and

K. T. Cheng
Argonne National Laboratory, Argonne, Illinois 60439

and

W. R. Johnson
Department of Physics, University of Notre Dame, Notre Dame, Indiana 46556

and

T. B. Lucatorto, T. J. McIlrath,(a) and J. Sugar
Center for Radiation Research, National Bureau of Standards, Washington, D.C. 20234

(Received 30 September 1982)

The first experimental-theoretical study of Rydberg autoionizing resonances along an isoelectronic sequence is presented. This analysis demonstrates the intimate connection between electron-electron correlation, term dependence, and autoionization and underscores the power of multichannel quantum-defect theory in analyzing complex spectra.

PACS numbers: 32.80.Dz, 32.30.Jc, 32.70.Jz

The combination of the recent development of multichannel quantum-defect theory (MQDT)[1] and the growing capabilities of precision laser spectroscopy has stimulated a renewed interest in the spectroscopy of Rydberg states. These states have provided a rich testing ground in which to refine our understanding of atomic structure,[2] of electric and magnetic field effects on atomic systems,[3] and on radiative interactions.[4] In this paper, we have analyzed the spectra of Xe and Ba^{++} with an empirical MQDT approach and combined this analysis with calculations based on the relativistic random-phase approximation (RRPA)[5] to explain how the changes related to the increasing nuclear charge can be used to reveal some fundamental relationships.

The Rydberg series observed from the $5p^6\,{}^1S_0$ ground state of a Xe-like system can be described in terms of five interacting channels (with $J=1$) which are conveniently labeled by the jj coupling scheme. We denote these channels by ${}^2P_{3/2}ns_{1/2}$, ${}^2P_{3/2}nd_{3/2}$, ${}^2P_{3/2}nd_{5/2}$, ${}^2P_{1/2}ns_{1/2}'$, and ${}^2P_{1/2}nd_{3/2}'$. The first three channels describe the three discrete (or bound) Rydberg series leading up to the $5p^5\,{}^2P_{3/2}$ (or I_1) limit. The fourth and fifth channels describe two series leading up to the second limit, $5p^5\,{}^2P_{1/2}$ (or I_2). The members of the latter two series which lie above I_1 are degenerate with the continuum states of the first three channels; this degeneracy is what gives rise to the autoionization observed between I_1 and I_2.

Figure 1 shows these (Beutler-Fano[7]) autoionizing resonances in a segment of the observed photoabsorption spectra of Xe and Ba^{++} as functions of the effective quantum number ν_2, defined by the relationship

$$E = I_2 - \zeta^2 \mathcal{R}/\nu_2^2, \tag{1}$$

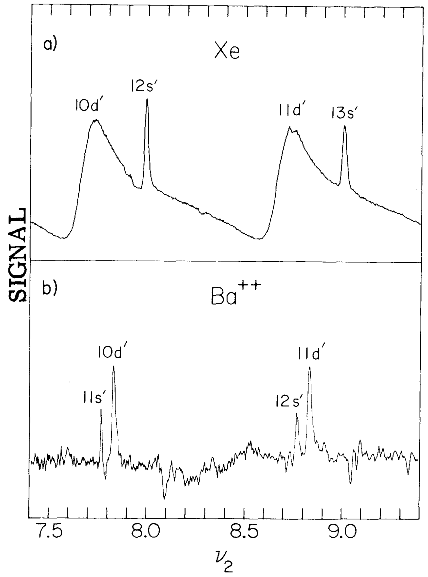

FIG. 1. Xe and Ba^{++} autoionizing resonances as a function of ν_2. (a) Photoelectron spectrum of Xe (Ref. 6). (b) Photoabsorption of Ba^{++}. The ζ^2 energy scaling implies a reduction of Ba^{++} width by a factor of 9 in ν_2 space; we observe a reduction of more than 18.

with $E = \hbar\omega$ being the incident photon energy, ζ the effective charge of the core, and $\mathcal{R}$ the Rydberg constant. The Ba^{++} spectrum was obtained by us with a new technique which employed two-stage laser-driven ionization to create a nearly homogeneous column of Ba^{++} ions suitable for photoabsorption measurements.[8] The Xe spectrum is well known, and the one shown in the figure was obtained by Eland in a conventional photoelectron experiment.[6]

Two striking differences between the Xe and Ba^{++} spectra are immediately apparent: the shift in the positions of the s' (and to a smaller degree the d') resonances and the marked decrease of the d' autoionizing widths in Ba^{++}. The shifts are related to the tendency of the energy levels in isoelectronic sequences to approach hydrogenic values as ζ increases. They have long been observed in emission spectra of bound Rydberg levels and will not be discussed here. Instead, we shall focus on the decrease of the d' autoionization widths.

Our discussion of resonance widths is based on MQDT which utilizes the scattering eigenstates of the system of core plus electron for a description of the Rydberg spectrum. The fundamental dynamical parameters are the phase shifts of the scattering eigenstates of the system (designated by $\pi\mu_\alpha$, where the μ_α's are defined as the eigenquantum defects), the unitary transformation matrix $U_{i\alpha}$ which connects the jj-coupled states designated by "i" and the scattering eigenstates designated by "α," and the eigenamplitudes, D_α, which are the dipole matrix elements between the ground state and the αth eigenstate. These parameters, μ_α, $U_{i\alpha}$, and D_α, which are slowly varying functions of energy, together with the position of the series limits form the basis for a complete description of the Rydberg spectrum.[1]

One of the powerful results of MQDT is that the two-dimensional Lu-Fano plot[9,10] contains most of the information needed to describe the Rydberg spectrum for a two-limit system (such as Xe, Cs^+, and Ba^{++}) in both the bound and autoionizing regions. The points on an empirical Lu-Fano plot are determined by assigning to each bound level a pair of effective quantum numbers ν_1 and ν_2, where ν_1 is defined relative to I_1 by an equation similar to Eq. (1). The points (ν_1,ν_2) are plotted with ν_1 (mod1) as the ordinate and ν_2 (mod1) as the abscissa, and a family of smooth, nonintersecting curves is drawn to connect the points. These curves define the quantum-defect functions, τ_ρ $(\rho = 1,2,3)$, which can be continued smoothly into the autoionizing region between I_1 and I_2 where the $\pi\tau_\rho$'s become the phase shifts of the three open scattering eigenchannels.

Figure 2 shows a single ν cycle of the autoionizing spectrum (which is nearly periodic in ν_2) for Xe, Cs^+, and Ba^{++} placed above the associated Lu-Fano plot. The points drawn on the Lu-Fano curves for Xe and Ba^{++} are taken from measurements[11] of the bound spectrum of those species. The theoretical results for Cs^+, calculated by the RRPA method,[5] are included to illustrate better the systematic changes in going along the isoelectronic sequence.

We now focus on the relationships between the Lu-Fano plot and the photoabsorption between I_1 and I_2. The occurrence of a resonance is accompanied by a unit increase in $\sum\tau_\rho$,[9,10] as can be clearly seen in Fig. 2. For Xe, near the d' resonance, the curves show a gradual slope which is associated with a broad resonance, while in Ba^{++} all of the curves have sharp, well-defined steps and the resonances are correspondingly narrow. Sharp, well-defined steps are observed near all s' resonances which are also narrow. The relationship between the τ_ρ curves and the autoionizing spectrum allows us to exploit certain properties of the Lu-Fano plot to describe the observed decrease in the d' resonance widths.

In the limiting case of no interaction between

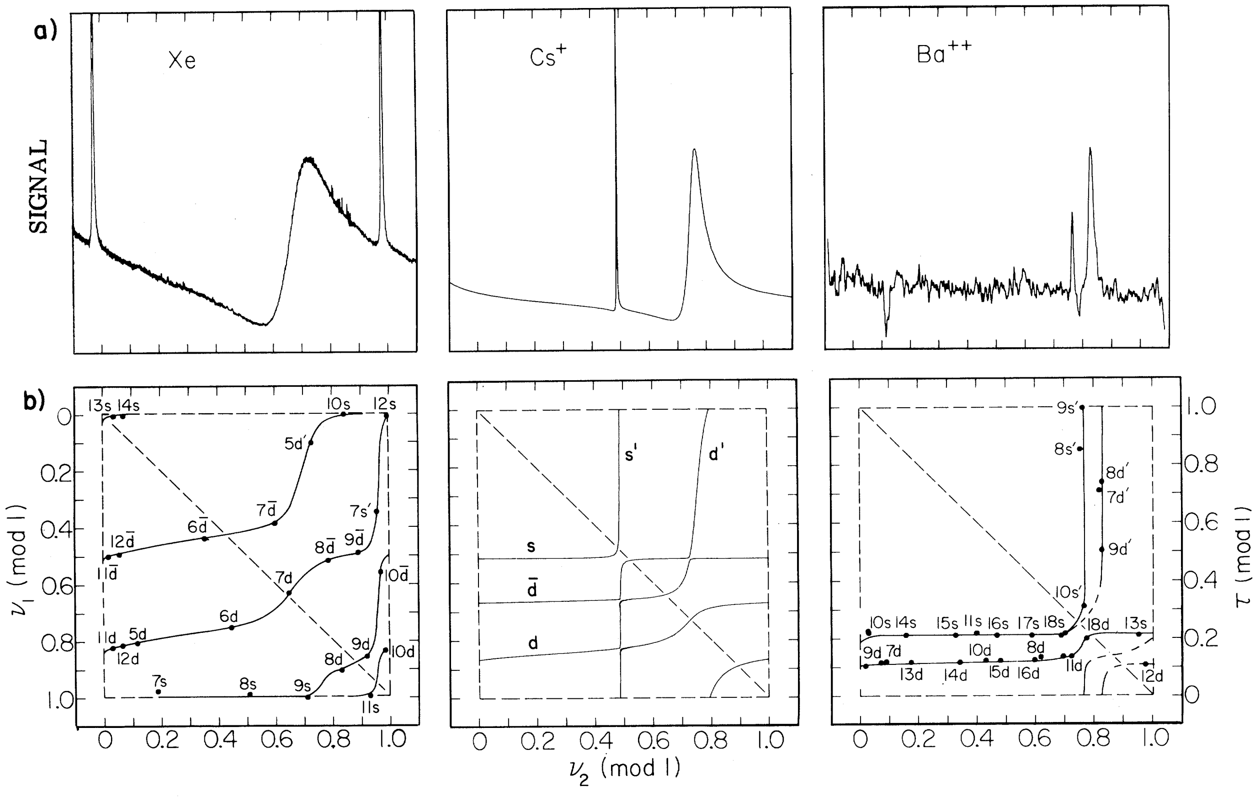

FIG. 2. One ν cycle of the Xe, Cs^+, and Ba^{++} spectra; (b) Lu-Fano plots of these spectra obtained from Ref. 11. The $d_{3/2}$ and $s_{1/2}$ levels (going to I_1) are unresolved in Ba^{++}; only the $s_{1/2}$ levels are denoted in the figure. The Cs^+ results are from our RRPA calculation.

the channels and no dependence of the MQDT parameters on energy, the Lu-Fano plot (of τ_p) would consist of three horizontal lines (constant ν_1) associated with the $^2P_{3/2}nl$ channels and two vertical lines (constant ν_2) associated with the $^2P_{1/2}nl'$ channels. Since there is always a residual interaction in any real case, a closer inspection near the points of possible intersection would show sharply avoided crossings. A situation of this type is shown in the Cs^+ Lu-Fano plot in the region near $\nu_2 = 0.5$, $\nu_1 = 0.65$ and 0.85. As the interaction between two channels increases so does the range and magnitude of repulsion in the avoided crossing between the corresponding curves. The τ_ρ curves for Ba^{++} are all characterized by narrow avoided crossings while those for Xe (i.e., near d' resonances) show wide avoided crossings. A similar connection has been pointed out in the analogous e-H scattering resonances by Macek.[12]

Autoionizing widths are thus closely related to the steepness of the steps in τ_ρ. In order to connect the differences between the Xe and Ba^{++} Lu-Fano plots to correlation effects, we must introduce one further result of MQDT: the intersection of a Lu-Fano τ_ρ curve with the diagonal, defined by $\nu_1(\mathrm{mod} 1) = \nu_2(\mathrm{mod} 1)$, gives the eigenquantum defect μ_α.[10] As can be seen in the progression of the Lu-Fano plots from Xe to Ba^{++}, the avoided crossings become narrower and approach the diagonal. As a consequence, the eigenquantum defects associated with an avoided crossing approach a common value. Our calculations show that the scattering eigenstates are nearly LS coupled for Xe, Cs^+, and Ba^{++}; we designate them as $(p^5s)^3P, {}^1P$ for $\alpha = 1, 2$ and $(p^5d)^3P, {}^3D, {}^1P$ for $\alpha = 3, 4, 5$. The experimental values of μ_α (for $\alpha = 1$–5), determined from the Lu-Fano plots, are as follow: Xe$\{1.05, 0.99, 0.54, 0.34, 0.18\}$; Ba^{++} $\{0.26, 0.21, 0.24, 0.17, 0.10\}$. (For comparison, the theoretical values are Xe$\{1.01, 0.94, 0.55, 0.32, 0.06\}$; Cs^+ $\{0.52, 0.48, 0.37, 0.28, 0.11\}$; Ba^{++} $\{0.21, 0.17, 0.19, 0.12, 0.05\}$.) It is obvious from the figure or the μ values that the difference between the p^5s eigenquantum defects (μ_1 and μ_2) are relatively small for Xe and decrease by a small amount in going from Xe to Ba^{++} while the differences between the p^5d defects (μ_3, μ_4, and

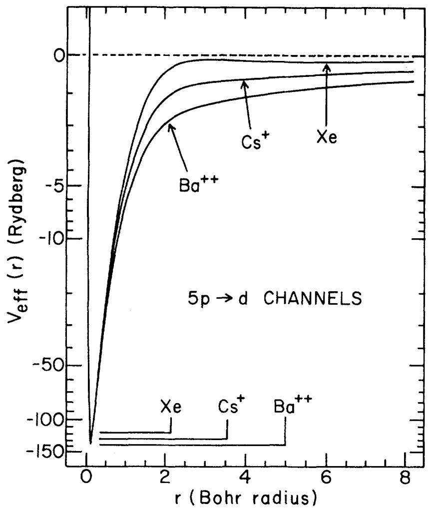

FIG. 3. Lowest-order RRPA calculation of the effective potential, V_{eff}, for $5p^5d$ channels of Xe, Ca$^+$, and Ba^{++}.

μ_5) are large for Xe and decrease dramatically in going from Xe to Ba^{++}. The smaller differences between the p^5d eigenquantum defects (which are proportional to the eigen phase shifts of the p^5d ^3P, ^3D, and ^1P channels) in Ba^{++} reflects a decrease in term dependence associated with the increase in effective nuclear charge.

To demonstrate how the eigenquantum defects are affected by changing correlation effects along the isoelectronic sequence, we calculated the effective potential for the p^5d channels. The coupled-channel equations used in RRPA are in general given by

$$(h + V_i - \epsilon)Y_i = \sum_j V_{ij} Y_j , \qquad (2)$$

where h is the single-particle Hamiltonian, V_i is the central potential for the excited orbital Y_i in the ith channel, and V_{ij} is the potential operator that couples the ith and the jth channels. In the lowest-order calculations where channel interactions are neglected [right-hand side set equal to 0 in Eq. (2)], electrons move in an effective potential V_{eff} arising from the central potential V_i and the centrifugal barrier $l(l+1)\hbar^2/2mr^2$. Addition of the diagonal channel-coupling terms $V_{ii}Y_i$, to account for intrachannel exchange, results in a term-dependent Dirac-Fock calculation while the additional coupling terms $V_{ij}Y_j$ account for interchannel correlation. It is the addition of these correlation effects which results in different eigenquantum defects for the five different channels. Conversely, the magnitude of the eigenquantum defect differences is a measure of the importance of correlation effects relative to the effective central potential.

In Fig. 3, the effective potential V_{eff} for the p^5d channels are shown for Xe, Cs$^+$, and Ba^{++}. The central potential V_i is the Dirac-Hartree potential for the ionic core; essentially it is the $V_{jj}^{(N-1)}$ potential discussed by Johnson and Lin.[13] One sees that there is a plateau in this effective potential for Xe, and that this plateau gradually disappears in the effective potentials of Cs$^+$ and Ba^{++}. The plateau in the effective potential of Xe arises from a near cancellation between the central potential and the centrifugal barrier in the valence region. The result is that the Xe$^+$ core is very sensitive to otherwise small perturbations due to channel correlations.

We have thus seen how amplified correlation effects enhance the term dependence of the wave functions of the LS eigenstates, subsequently leading to large eigenquantum defect differences in Xe. As the central potential becomes more dominant with increasing core charge, the eigenquantum defect differences decrease in Cs$^+$ and Ba^{++}. The decreasing autoionization widths with increasing core charge are thus viewed to be a consequence of the increasing importance of the nuclear term of the central potential. By contrast, there is no centrifugal barrier in the p^5s channels; the eigen phase shift difference between the excited s orbitals is always small (hence, so are the autoionization widths) and varies little along the isoelectronic sequence.

We thank J. Berkowitz for his unpublished Xe data and U. Fano, C. W. Clark, M. L. Ginter, W. Martin, and R. P. Madden for helpful discussions. This work was supported in part by National Science Foundation Grants No. CPE 7918 387A01 and No. PHY8107382 and U. S. Department of Energy Grant No. W-31-109-ENG-38. One of us (W.T.H.) was the recipient of a Naval Research Center–National Bureau of Standards Fellowship.

---

[a] Permanent address: Institute for Physical Science and Technology, University of Maryland, College Park, Md. 20742.

[1] U. Fano, J. Opt. Soc. Am. 65, 979 (1975); M. J. Seaton, J. Phys. B 11, 4067 (1978); C.-M. Lee and W. R. Johnson, Phys. Rev. A 22, 979 (1980).

[2] R. Beigang, E. Matthias, and A. Timmerman, Phys. Rev. Lett. 47, 326 (1981); C. M. Huang and C. C. Wang, Phys. Rev. Lett. 46, 1195 (1981).

[3] T. S. Luk, L. DiMauro, T. Bergeman, and H. Met-

calf, Phys. Rev. Lett. 47, 83 (1981); J. C. Gay, D. Delande, and F. Biraben, J. Phys. B 13, L729 (1980).

[4] D. Kleppner, Phys. Rev. Lett. 47, 233 (1981); A. G. Vaidyanathan, W. P. Spencer, and D. Kleppner, Phys. Rev. Lett. 47, 1592 (1981).

[5] W. R. Johnson, K. T. Cheng, K.-N. Huang, and M. LeDourneuf, Phys. Rev. A 22, 989 (1980).

[6] J. Berkowitz, personal communication; see also Ref. 5.

[7] H. Beutler, Z. Phys. 93, 177 (1935); U. Fano, Nuovo Cimento 12, 156 (1935).

[8] T. B. Lucatorto and T. J. McIlrath, Appl. Opt. 19, 3948 (1980).

[9] U. Fano, Phys. Rev. A 2, 353 (1970).

[10] K. T. Lu, Phys. Rev. A 4, 579 (1971); C.-M. Lee and K. T. Lu, Phys. Rev. A 8, 1241 (1973).

[11] The experimental points of the bound Xe spectrum are from C. E. Moore, *Atomic Energy Levels*, U. S. National Bureau of Standards Circular No. 467 (U.S. GPO, Washington, D.C., 1971); the points for Ba^{++} are from W. T. Hill *et al.*, to be published.

[12] J. Macek, Phys. Rev. A 2, 1101 (1970).

[13] W. R. Johnson and C. D. Lin, Phys. Rev. A 20, 964 (1979).